Numerical and experimental study of the load of an object due to the effects of a flow field in the atmospheric boundary layer

Vladimira Michalcova, Sergej Kuznetsov, and Stanislav Pospisil

***Abstract*—**This paper describes a comparison of two different solutions of a standard problem in building aerodynamics, i.e. the load of a cube-shaped object exposed to the effects of an air flow field. Two problems are discussed in this article. First is the solution of the flow field with the constant wind velocity and low turbulence intensity, while the second problem is about the flow in the simulated atmospheric boundary layer, i.e. the flow field with the high intensity of the turbulence and with the gradient velocity. Physical modelling takes place in the climatic wind tunnel of the Institute of Theoretic and Applied Mechanics AS CR in Telč and numerical modelling is solved using the Ansys Fluent software at the Faculty of Civil Engineering of VŠB – Technical University of Ostrava.

***Keywords*—** atmospheric boundary layer (ABL), bluff body, CFD, ELES, SAS, wind tunnel.

I. Introduction

Modelling a flow around low objects of non-aerodynamic shapes brings many problems [1], [2] and this applies to both numerical and physical simulations. The aim of the paper is to compare results of the physical and numerical modelling of an air-flow around an object of the shape of a cube with an edge of 0.24 m. It represents the so-called Silsoe cube with a scale of 1:25 that has gradually become a standardized experimental element in the field of building aerodynamics. The reason for this choice is the possibility of using informative data from measurement in the tunnel to assess the final results of both approaches [3], [4].

A flow field was modelled within a physical experiment in the CET wind laboratory http://cet.arcchip.cz/. Turbulence intensity i is defined as the ratio between standard deviation of the fluctuation part to the mean velocity. Furthermore, the flow field has been compared with the numerical model created within the Ansys-Fluent numerical code. The object of evaluation is the pressure load of the model due to the effects of a flow field. If is defined here using the dimensionless external pressure coefficient c_{pe} that is the ratio of the static pressure and the dynamic pressure related to the reference point:

$$c_{pe,i} = \frac{p_i}{p_{dyn}} = \frac{p_{ci} - p_{ref}}{1/2 \cdot \rho \cdot u_{ref}^2}, \tag{1}$$

where:

p_{ref} is the static pressure at the reference point [Pa];

p_{ci} is the resulting static pressure on the surface of the object at the i-th point [Pa];

p is the static pressure on the surface of the object at the i-th point recalculated in relation to the reference pressure [Pa];

u_{ref} is the x-component of velocity at the reference point [m.s^{-1}]; and

ρ is the air density ρ=1.225 [kg.m^{-3}].

The external pressure coefficient c_{pe} has been measured, calculated, and evaluated in two sections perpendicular to each other and in a horizontal section. The scheme of the model with 30 sampling points is shown in Figure 1**.**

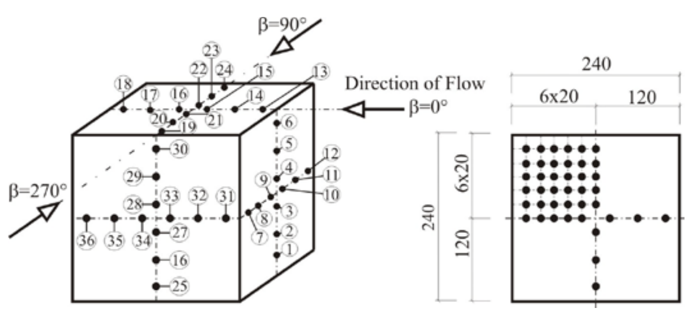

Fig. 1 Scheme of the model with the measurement points

The work is supported from funds of the conceptual development of science, research and innovation for 2013 allocated to the VŠB-Technical University of Ostrava by the Ministry of Education, Youth and Sports of the Czech Republic.

This paper was prepared with the support of the project CZ.1.05/1.1.00/02.0060 that is co-funded from the European Regional Development Fund.

Vladimíra Michalcová, VŠB-Technical University of Ostrava, Faculty of Civil Engineering, Ludvíka Podéště 1875/17, 708 33 Ostrava - Poruba, Czech Republic, e-mail: vladimira.michalcova@vsb.cz.

Sergii Kuznetsov, ÚTAM AV ČR, v.v.i. Centrum excelence Telč, Batelovská 485, Telč, Czech Republic e-mail: kuznetsov@itam.cas.cz.

Stanislav Pospíšil, VŠB-Technical University of Ostrava, Faculty of Civil Engineering, Ludvíka Podéště 1875/17, 708 33 Ostrava - Poruba, Czech Republic, e-mail: pospisil@vsb.cz.

II. PHYSICAL EXPERIMENT

The experiments were carried out in the climatic wind tunnel of the Centre of Excellence Telč, the Institute of Theoretical and Applied Mechanics of the AS CR. The testing section of the aerodynamic section has a rectangular cross-section of 1.9 m (width) × 1.8 m (height). The total length of the coming flow part of the aerodynamic section is 11.0 m, including the turbulent boundary layer development part with 9 m of length. If necessary, a simulation of the atmospheric boundary layer with the required characteristics is modelled using elements such as networks, so-called Counihan's generators, barriers, and floor plates with different roughness.

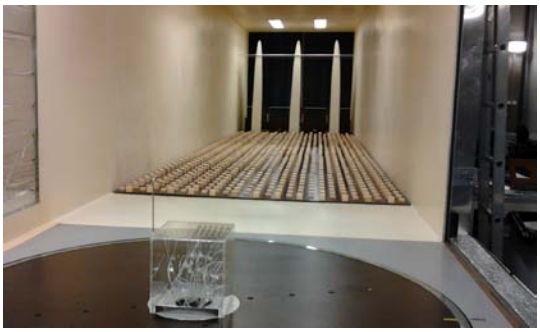

Fig. 2 The model in the measuring-aerodynamic section

The model of a cube was placed in the centre of the rotary table (with a diameter of 1.76 m) in the work part of the aerodynamic section of the tunnel (Fig. 2). The cube was made of transparent Plexiglass with a wall thickness of 5 mm; the drainage points have a diameter of 0.5 mm and are equipped with connectors in the shape of a metal tube with an inside diameter of 1 mm. All connectors of the drainage points are connected using a silicone tube (with a length of 1 m and a diameter of 2 mm) with the measuring device Scanivalve Corp. DSA 3217 for sensing the pressure. The data and conversion to digital values were collected in the acquisition system (DEWETRON) with the sampling frequency equal to 1 kHz.

The results of the pressure coefficients are shown as the function of air flow direction $\beta = 0\ldots360°$ and can be recorded as $c_{pe,i}=f(\beta)$. The interval of model rotation on the vertical axis $\Delta\beta$ was 90°.

A. *The smooth flow field with a constant vertical velocity*

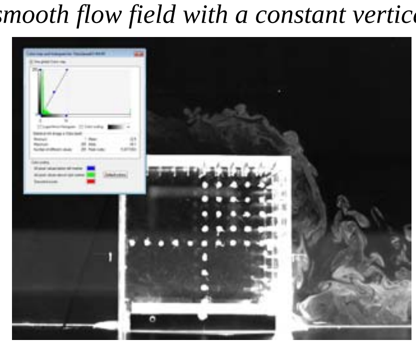

Fig. 3 The flow around the model in the aerodynamic section

The experiments were carried out with Reynolds number $Re = 2.1\cdot10^5$ [-] that corresponded to an air flow velocity of 13.5 m/s (Fig. 3).

Figure 4 shows the values of the pressure load on the axis of the upper wall when the cube was rotated through 0°, 90°, 180°, and 270°. The coefficient c_{pe} at points of the corresponding longitudinal axis in the direction of flow was defined on each rotation.

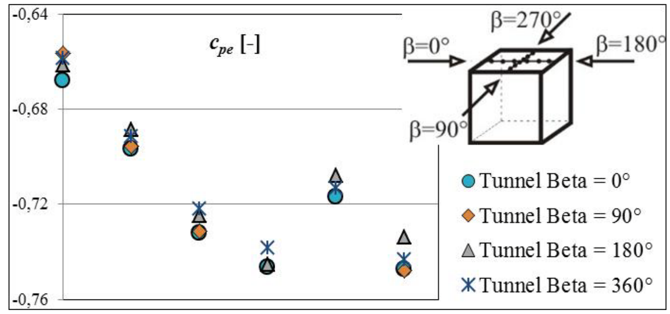

Fig. 4 Detail of the upper wall longitudinal axis load values for various angles of rotation of the cube

B. *The flow field with the high intensity of the turbulence and with the gradient velocity-ABL flow*

The flow around the model in the field with the high intensity of the turbulence and with the approaching flow velocity with the gradient corresponding to the suburban terrain (see Fig. 4). The experiment were carried out with the Reynolds numbers $Re = 0.8\cdot10^5$ [-], $1.1\cdot10^5$ [-], and $1.4\cdot10^5$ [-], respectively. This corresponds to the respective reference flow velocities $u_{ref\,1} = 5.5$ m.s^{-1}; $u_{ref\,2} = 7.65$ m.s^{-1} and $u_{ref\,3} = 10.2$ m.s^{-1} in the empty measuring section (no model). Reference height $z_{ref} = 0.24$ m is equal to the top edge of the cube.

III. NUMERICAL MODELLING

Numerical models suitable for this type of problem can be divided into two categories:

- RANS models and
- models for anisotropic turbulence – RSM and LES and its combinations with RANS models.

RANS models. These are statistical turbulence models that are based on the method of the time-averaging (Reynolds Averaged Navier-Stokes equations) of turbulent flow variables and on the following procedure for time-averaging balance equations describing a turbulent flow. They use so-called Boussinesq's hypothesis that uses a simplified expression of Reynolds stresses. To calculate the problem, the Spalart Allmaras, Standard k-ε, RNG k-εrch, and SST k-ω models were used respectively. They are based on isotropic turbulence modelling. They differ from each other in defining the so-called turbulent dynamic viscosity, a variable that expresses complex functional relations of the state of a flowing fluid and the position of a point being considered. An advantage of RANS models is the lower requirements for the calculation of the area grid density, the possibility of modelling a stationary problem, and the ability to make a rapid calculation. Unfortunately, they are less suitable for solving a flow around structures of non-aerodynamic shapes because strong anisotropic turbulence is created in the surroundings of the object. A calculation area of a size of 1.9 m (width) × 1.8 m (height) × 4.5 m (length) was created for RANS models.

The monitored object was placed at a distance of 1m from the entrance to the domain. $1x10^6$ tetra cells are used to create the mesh of the examined domain according to Fig. 5 to the left, in which the high density in the surroundings of the object as well as the uniform longitudinal strip required for solving correctly the boundary condition on the side walls are apparent.

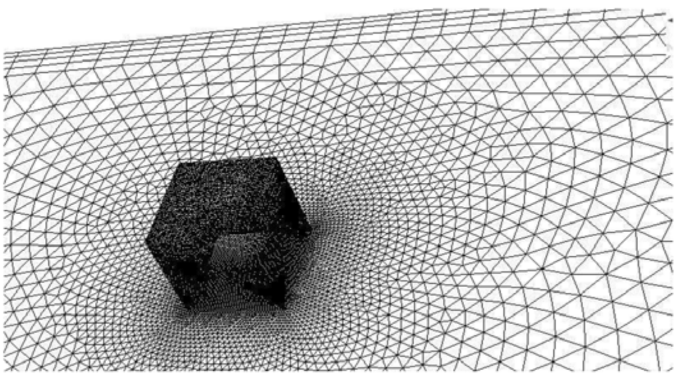

Fig. 5 Tetra grid for the RANS and SAS models: Horizontal plane in the middle of the height of the object

Models for anisotropic turbulence. These models are based on the principle of modelling anisotropic turbulence, which better reflects the examined action. However, they require higher quality and density of the mesh and the problems must be solved in a non-stationary way, so that the computational times are significantly longer. An exception is the RSM model. It enables to solve a problem in a stationary way, but it is very sensitive and frequent problems with convergence occur when it is used. It was not used for the calculations presented here. Newly developed hybrid models that are a combination of the LES [5] and RANS methods, namely the SAS and ELES models, were used to solve the problem. Their correct combination enables to reduce significantly the number of cells in the calculation area and thereby reduce significantly the computational time, even though the transmission of variables at the interface of the areas also partially extends the computational time.

ELES models large vortex structures in the disordered flow field area (in this case the surroundings of the object being flowed around) using a direct simulation (LES) and in the area in which an ordered isotropic flow can be expected using the RANS method. It requires the precise definition of the interface, which allows for preparing meshing better. A new calculation domain with the dimensions 1.9m (width) × 1.8 m (height) × 5.0 m (length) with combined grids (Fig. 6) was created for this calculation. The base is a polyhedral cell. The defined domain in the surroundings of the object for a direct simulation using the LES method then consists of a thick grid of the hexagonal cells. This domain with a length of 1m begins at the distance at 0.2 m in front of the object and its transverse dimensions exceed the perimeter of the cube being flowed around by 0.2 m on each of its sides. Figure 6 shows the difference in the density of the grid as well as the tendency how the sizes of the polyhedral cells gradually increase with the increasing distance from the object.

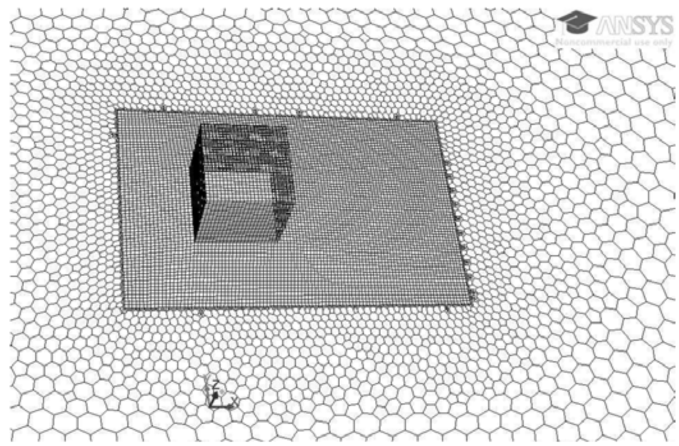

Fig. 6 Combined grid for the ELES model

The SAS model defines the interface on the basis of the linear scale of vortices and behaves as the SST k-ω model in close proximity to the wall and switches automatically to the LES calculation at a larger distance. Its limits do not need to be entered. The calculation area was the same as that for the RANS models for the calculation.

Vortex structures of the surroundings of the object using the ELES model see Fig. 7.

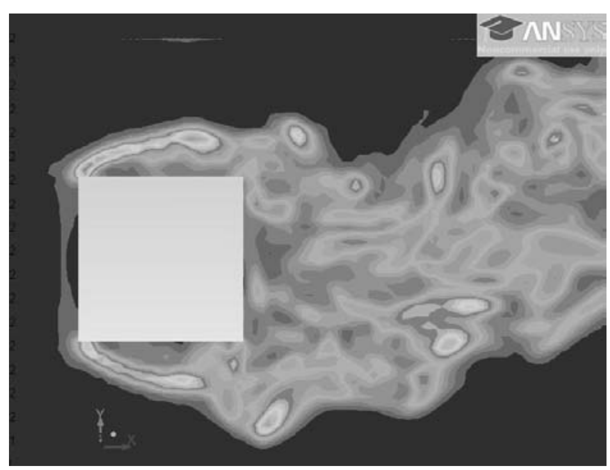

Fig. 7 Vortex structures of the surroundings of the object

A. Boundary conditions- the smooth flow field with a constant vertical velocity

The same types of boundary conditions were set for all calculations. These are the velocity at the inlet and the pressure-outlet condition at the outlet of the calculation domain. The bottom surface is presented using the wall condition, which is the same as in the case of modelling of the open space (atmosphere). The boundary conditions on both sides and on the upper surface of the calculated domain were defined using the wall to correspond to the bounded space of the tunnel, which requires additional requirements on the shape of the grid, the aforementioned uniform distribution of a certain density in the surroundings of the walls.

B. Boundary conditions- the flow field with the high intensity of the turbulence and with the gradient velocity

The flow with the turbulence intensity describing the wind in the Atmospheric Boundary Layer was calculated by the ELES method only that showed the best results in the flow field with the constant velocity (see below). The reference wind velocity was $u_{ref} = 10.2\ \mathrm{ms}^{-1}$. The wind velocity gradient at the edge of the calculation domain has been defined by the commonly used power law profile corresponding to the modelled terrain:

$$u = u_{ref} \cdot \left(\frac{z}{z_{ref}} \right)^{0,22} \quad \left[\ \mathrm{m.s}^{-1} \right], \tag{2}$$

Other parameters used in the calculation were defined:

friction velocity:

$$v* = \frac{\kappa \cdot u_{ref}}{\ln\left(\left(z_{ref} + z_0 \right) / z_0 \right)} \quad \left[\ \mathrm{m.s}^{-1} \right], \tag{3}$$

kinetic energy:

$$k = \frac{v*^2}{0.3} \quad \left[\ \mathrm{m}^2.\mathrm{s}^{-2} \right], \tag{4}$$

and the kinetic energy dissipation parameter:

$$\varepsilon = \frac{v*^3}{\kappa \cdot \left(z + z_0 \right)} \quad \left[\ \mathrm{m}^2.\mathrm{s}^{-3} \right], \tag{5}$$

where:

u_{ref} is the reference velocity in the height
z_{ref} above the terrain $[\mathrm{m.s}^{-1}]$,
z_{ref} reference height (cube top edge elevation), $z_{ref} = 0.24$ m,
z height above the terrain [m],
κ von Kármán constant $\kappa = 0.419$ [-] ,
z_0 aerodynamic roughness, in this case $z_0 = 0.005$ m.

IV. RESULTS

The external pressure coefficient on the cube was measured, calculated, and evaluated in two vertical sections (see Fig. 8, 9 and 12,13) perpendicular to each other and in a horizontal section (see Fig. 10 and 14).

A. The smooth flow field with a constant vertical velocity

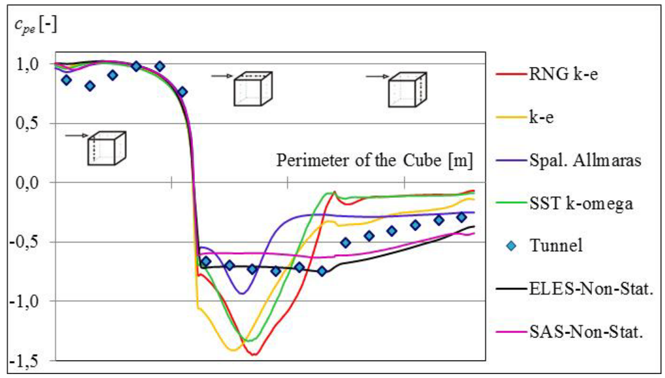

Fig. 8 Vertical longitudinal section, smooth flow

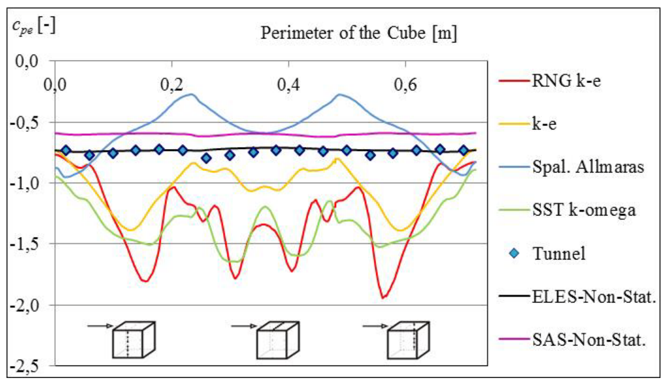

Fig. 9 Vertical cross section, smooth flow

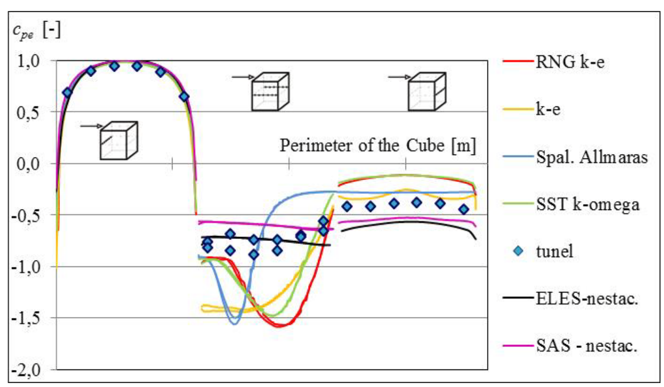

Fig. 10 Horizontal section, smooth flow

For the calculation using the ELES model, the instantaneous static pressure on the upper wall of the object at points corresponding to sampling points 13 and 18 and also in the center of the wall was recorded. The values of the instantaneous static pressure at individual time steps in par. 18 are in the Figure 11.

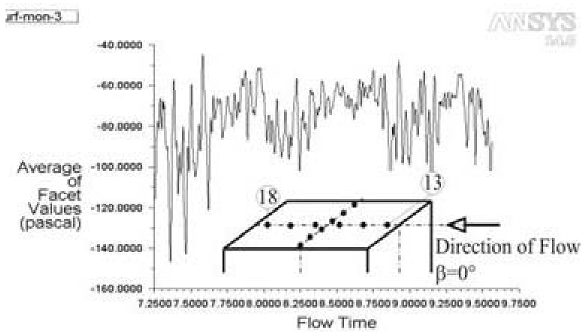

Fig. 11 Instantaneous static pressure at point 18 when calculated using the ELES model

B. The flow field with the high intensity of the turbulence and with the gradient velocity

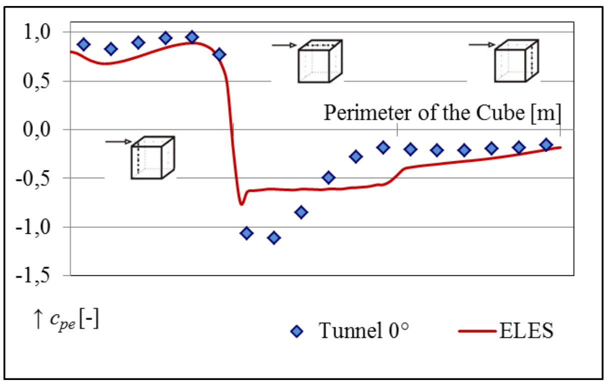

Fig. 12 Vertical longitudinal section, ABL flow

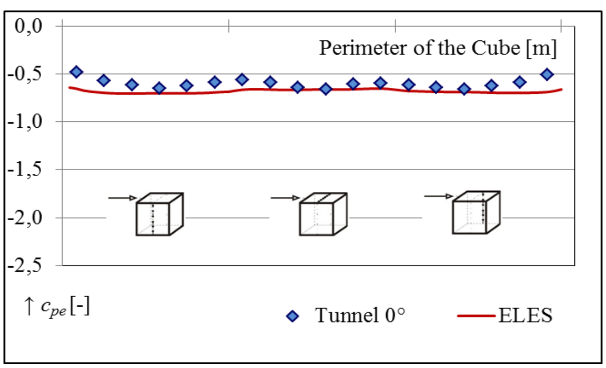

Fig. 13 Vertical cross section, ABL flow

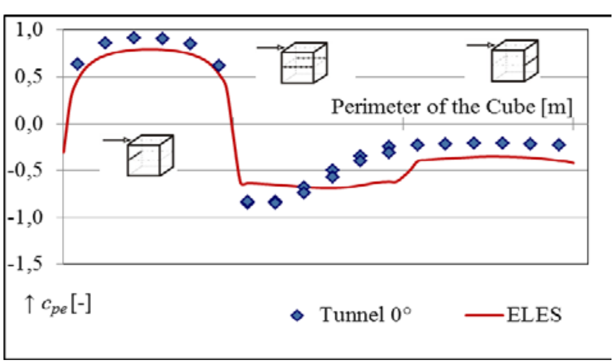

Fig. 14 Horizontal section, ABL flow

V. Evaluation of Numerical Modelling

A. The smooth flow field with a constant vertical velocity

The RANS models appears to be unsuitable for this type of problem because strong anisotropic turbulence arises especially on the sides and on the leeward side of the object in its close vicinity.

On the front side, where no strong vortex occurs, all calculations agree with the wind tunnel experimental measurement. There are marked differences in the results of the pressure load along the object, i.e. on the sides and on the upper wall. The load in the vertical lateral section proves the unsuitability of RANS models for the description of the flow field. For the leeward side of the object, the results from the Standard k-ε and the Spalart Allmaras models are the closest ones to the experimental results.

Also the ELES and SAS non-stationary models produced satisfactory results. Moreover, the ELES model gave the results on the front, the upper and the both sides almost identical to those measured in the wind tunnel. The results on the leeward side differ slightly.

The SAS model correctly copies the shape of the load curve along all three monitored perimeters of the cube being flowed around. A small displacement could be avoided by using a more dense grid and longer simulated time of the flow. This will be in the focus of the next analysis.

B. The flow field with the high intensity of the turbulence and with the gradient velocity

Due to high turbulence, the pressure distribution on the surface of an object, especially on the upper side changes. The numerical model appeared to be non-sufficient to capture this feature and thus needs to be developed and tested. The problem could occur when the variables cross the interface areas. The solution could be improved by the increase of the mesh density in the vicinity of the object, where the LES method is employed. This, however, will lead to higher demands on the computational time.

A disadvantage of the non-stationary calculations is their demands from the viewpoint of the preparation of calculation (the shape and density of the calculation mesh and the correct definition of a time step) as well as its time-consuming nature. For both non-stationary problems, a time step of 0.001 second was selected and the calculation simulated a flow for 4 seconds, with the averaging of the variables carried out after 1 second of the simulated action. At that time, it was possible to regard the flow field as a steady one. The resulting time of the flow with the time-averaging of the variables represented approximately eight times the air exchange in the calculation area. There were approx. $4{\cdot}10^4$ iterations within one calculation.

Is worthy to consider future analysis by using the approach, described in [6], [7].which is based on the turbulence elements created at ground of the inlet part of the computational domain. This would substitute the RANS method used so far, which is unable to generate the turbulence.

VI. Evaluation the Experiment

The unchanging values of the measured pressure load at the defined points when the cube was sequentially rotated (see Fig. 3 and 15) contribute to the positive evaluation.

There proved to be a difference when the load in the horizontal section was evaluated; the load values on the axes of the left and right sides differed slightly from each other, see (Fig. 10) as well as (Fig. 15) for the detail. Considering the slight asymmetry of the horizontal load of the front wall, this could be caused by the small deflection of the flow or the rotation of the monitored object, which also corresponds to the delicately asymmetric load side walls (Fig. 16). This will be the subject of additional measurement.

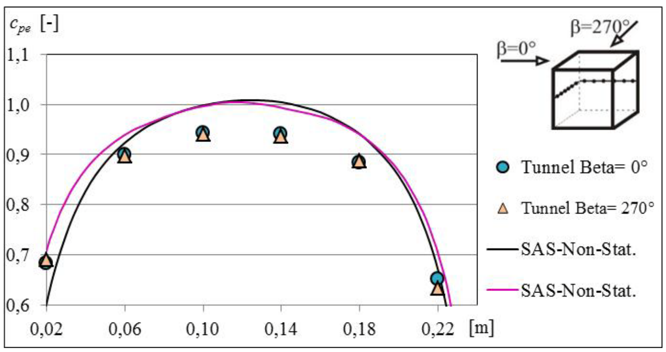

Fig. 15 Detail of the front wall horizontal axis load values for various angles of rotation of the cube

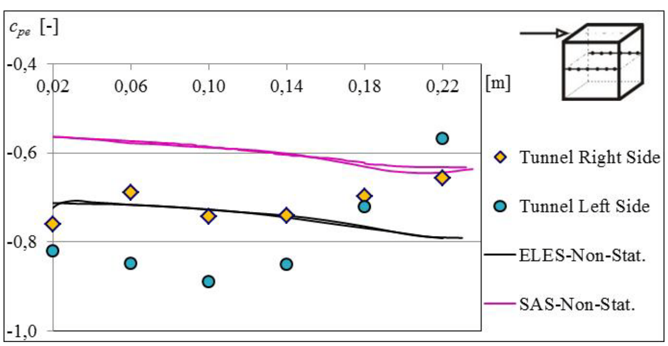

Fig. 16 Detail of the side wall longitudinal axis load values

VII. Conclusion

The solution of this problem proved that a flow around an object of non-aerodynamic shape is a complex action for modelling, whether experimental or mathematical one, and that mutual cooperation between the two approaches is necessary. Same is true in other research fields, such as [8], [9].

The results of the numerical simulations using ELES and SAS models for non-stationary problems in the calculation of smooth flow showed a very satisfactory similarity with the experiment, which is promising for the further modelling the ABL flow-flow field with the high intensity of the turbulence and with the gradient velocity. For the solution of the wind load in the ABL, the authors will focus both on the use of high lever experimental tools (e.g. PIV, 3D anemometry) for the turbulence determination and on the solution of the modelling and maintaining the higher turbulence in RANS models.

The correct methodology of numerical modelling of highly turbulent flow in the ABL will also contribute to solving problems in environmental issues [10] or energy [11].

References

[1] Y. Q. Zhang, A. H. Huber, S. P. S. Arya, and W. H. Snyder, “Numerical simulation to determine the effects of incident wind shear and turbulence level on the flow around a building”, *Journal of Wind Engineering and Industrial Aerodynamics: Proceedings of the 1st International Conference on Computational Wind Engineering*. Vol.93, iss. 46-47, pp. 129-134.

[2] Y. Q. Zhang, and A. M. Gu, “Wind tunnel test and numerical simulations of wind pressures on buildings in staggered arrangement,” *Journal of Wind Engineering and Industrial Aerodynamics: The 4th International Symposium on Computational Wind Engineering.* vol.96, iss. 10-11, pp. 2067-2079.

[3] P. J. Richards, R. P. Hoxey, B. D. Connell, and D. P. Lander, “Wind-tunnel modelling of the Silsoe Cube,” *Journal of Wind Engineering and Industrial Aerodynamics: The 4th European and African Conference on Wind Engineering*. Vol. 95, iss. 9-11, pp. 1384-1399. ISSN 0167-6105.

[4] R.P. Hoxey, A. P. Robertson, and P. J. Richards “How have full-scale measurements improved the reliability of wind-loading codes,” *Journal of Wind Engineering:* 11th *International Conf. on Wind Engineering*, Lubbock, Texas, USA, 2003.

[5] T. Tamura, A. Okuno, and Y. Sugio, “LES analysis of turbulent boundary layer over steep hill covered with vegetation,” *Journal of Wind Engineering and Industrial Aerodynamics: The Fourth European and African Conference on Wind Engineering*. Vol. 95, iss. 9-11, ISSN 0167-6105.

[6] G. Knapp, N. Wright, and J. Owen “Comparsion of Full-Scale and CFD Results for the Silsoe 6m Cube,” *Journal of Wind Engineering*: 11th *International Conf. on Wind Engineering, Lubbock, Texas, USA*, 2003.

[7] K. Nozawa, and T. Tamura, “Large eddy simulation of wind over large roughness elements,” *Journal of Wind Engineering and Industrial Aerodynamics: The 4th European and African Conference on Wind Engineering*. Vol. 95, iss. 9-11. ISSN 0167-6105.

[8] L. Lausová, I. Skotnicová, I. Kološ, and M. Krejsa, “Experimental and numerical studies of the effect of high temperature to the steel structure (Published Conference Proceedings style),” in *Proc. 18th WSEAS International Conference on Applied Mathematics (AMATH´13)*, Budapest, Hungary, 2013, pp. 102–108, ISSN 2227-4588, ISBN 978-960-474-351-3.

[9] I. Skotnicová, P. Týmová, Z. Galda, and L. Lausová, “Numerical analysis and experimental validation of the thermal response of light weight frame structures (Published Conference Proceedings style),” in *Proc. 18th WSEAS International Conference on Applied Mathematics (AMATH´13)*, Budapest, Hungary, 2013, pp. 178–182, ISSN 2227-4588, ISBN 978-960-474-351-3.

[10] A. Askarova, S. Bolegenova, A. Maximov, and M. Beketayeva, “Research of the combustion of low-grade Kazakhstan coal in combustion chamber of the real energy facility,” *International Journal of Energy and Environment*, North Atlantic University Union, Vol. 7, iss. 2, pp. 64-73. ISSN 2308-1007.

[11] A. Ait-Alla, M. Quandt, and M. Lútjen “Simulatin-based aggregate Installation Planning of Offshore Wind Farms,” *International Journal of Energy and Environment*, North Atlantic University Union, Vol. 7, iss. 2, pp. 23-30. ISSN 1998-4316.